Geochemistry Geophysics Geosystems G3
AN ELECTRONIC JOURNAL OF THE EARTH SCIENCES
Published by AGU and the Geochemical Society

Data Brief
Volume 1
November 15, 2000
Paper number 2000GC000089
ISSN: 1525-2027

New experimental observations on the anhydrous solidus for peridotite KLB-1

Claude Herzberg
Department of Geological Sciences, Rutgers University, New Brunswick, New Jersey 08903 (herzberg@rci.rutgers.edu)

Also at Center for High Pressure Research and Mineral Physics Institute, State University of New York at Stony Brook, Stony Brook, New York 11794

Paul Raterron
Laboratoire de Structure et Propriété de l'État Solide, Université des Sciences et Technologies de Lille, Villeneuve d'Ascq, F-59655 Cedex, France

On leave at Center for High Pressure Research and Mineral Physics Institute, State University of New York at Stony Brook, Stony Brook, New York 11794 (raterron@sbmp04.ess.sunysb.edu)

Jianzhong Zhang
Center for High Pressure Research and Mineral Physics Institute, State University of New York at Stony Brook, Stony Brook, New York 11794 (zhang@sbmp04.ess.sunysb.edu)

[1] **Abstract:** New multianvil experimental data are reported for the anhydrous solidus for peridotite KLB-1 at 5 to 9.7 GPa. The solidus is unaffected by variable experimental run durations, but it is lowered in temperature when rhenium capsules are replaced with graphite. Using data reported previously, the anhydrous solidus for KLB-1 can be described by $T = 1086 - 5.7P + 390 \ln P$ (±68°C 2σ) at pressures that range from 2.7 to 22.5 GPa. At lower pressures the effect of composition on the temperature of the spinel peridotite solidus is small and dominated by alkali abundances; variations in Mg number have almost no effect on solidus temperature.

Keywords: Peridotite solidus; anhydrous initial melting.

Index terms: Igneous petrology; experimental mineralogy and petrology; high-pressure behavior.

Received June 22, 2000; **Accepted** October 5, 2000; **Published** November 15, 2000.

Herzberg, C., P. Raterron, and J. Zhang, 2000. New experimental observations on the anhydrous solidus for peridotite KLB-1, *Geochem. Geophys. Geosyst.*, vol. 1, Paper number 2000GC000089 [4498 words, 7 figures, 4 tables]. Published November 15, 2000.

Theme: Phase Relations and Trace Element Partitioning on the Mantle Solidus
Guest Editors: Vincent Salters and Jon Blundy

Table 1. Experimental Peridotite Compositions

	KLB-1[a]	KLB-1[b]	Kettle R[c]	Kettle R[d]	MPY[e]	TL[e]	MM3[f]	HK-66[g]	DW[h]	PHN 1611[i]
SiO_2	44.48	44.3	44.9	44.9	45.9	45.4	45.5	48.02	44.4	43.7
TiO_2	0.16	0.12	0.16	0.16	0.17	0.1	0.11	0.22	0.14	0.25
Al_2O_3	3.59	3.54	4.26	4.26	4.65	3.53	3.98	4.88	3.02	2.75
Cr_2O_3	0.31	-	0.41	0.41	0.57	0.26	0.68	0.25	0.76	0.28
FeOt	8.1	8.59	8.02	8.02	6.15	7.74	7.18	9.9	17.9	10.05
MnO	0.12	0.14	0.13	0.13	-	-	0.13	0.14	0.46	0.13
MgO	39.22	39.5	37.3	38.12	38.4	39.7	38.3	32.35	30.2	37.22
CaO	3.44	3.03	3.45	3.45	3.61	3.11	3.57	2.97	2.45	3.26
Na_2O	0.3	0.3	0.22	0.22	0.5	0.25	0.31	0.66	0.5	0.33
K_2O	0.02	0.01	0.09	0.09	-	-	-	0.07	-	0.14
NiO	0.25	-	0.24	0.25	-	-	0.23	-	-	-
Total	99.99	99.53	99.18	100	99.95	100.09	99.99	99.53	99.99	98.25
Mg #	89.6	89.1	89.2	89.4	91.8	90.1	90.5	85.3	75.0	86.8

[a] *Takahashi* [1986]; 0.206 is the sum of squares of residuals to phase compositions reported by *Takahashi* [1986].
[b] *Herzberg et al.* [1990]; 0.006 is the sum of residuals to phase compositions reported by *Takahashi* [1986].
[c] KR-4003 Kettle River Peridotite; *Walter* [1998].
[d] Walter compositions with MgO raised to total 100 (C. Herzberg, manuscript in preparation, 2000).
[e] MPY, MORB Pyrolite; TL, Tinaquillo Lherzolite: *Robinson et al.* [1998] at 1.5 GPa.
[f] *Baker and Stolper* [1994].
[g] *Takahashi and Kushiro* [1983].
[h] DW, Dreibus and Wanke mantle composition for Mars [*Bertka and Holloway*, 1994].
[i] *Kushiro* [1996].

1. Introduction

[2] The anhydrous solidus reported by *Walter* [1998] on Kettle River peridotite (KR-4003) at 5 GPa is ~100°C lower than the solidus for KLB-1 peridotite [*Zhang and Herzberg*, 1994; *Herzberg and Zhang*, 1996; *Iwamori et al.*, 1995], despite the fact that their compositions are similar (Table 1). We have therefore attempted to evaluate the cause of this discrepancy by reproducing experiments on KLB-1 at 5.0 to 9.7 GPa. The new results have enabled an assessment to be made of experimental precision and accuracy in multianvil melting experiments and of the effects of variations in experimental method. In order to place this information in the context of a low-pressure reference frame an examination is made of solidus determinations at 1 atm to 3 GPa from published piston-cylinder experiments. We begin this paper with a brief evaluation of the low-pressure data, and this is followed by a reporting of our new data for KLB-1. Our conclusions regarding the magnitude of experimental uncertainty, the effects of bulk peridotite composition on solidus temperature, and the choice of the most geologically appropriate anhydrous solidus are very similar to those that have been independently drawn by *Hirschmann* [2000] from a larger data set. However, we restrict this contribution to a data brief and encourage the reader to consult the *Hirschmann* [2000] paper for a comprehensive discussion and evaluation of existing data.

2. Experimental Peridotite Solidus at 1 atm to 3 GPa

[3] The peridotite solidus is bracketed by experimentally observing the presence and absence of glass or the crystalline quench products of liquid. Experimental brackets have been provided by *Takahashi* [1986] and *Falloon et al.* [1999] on peridotite

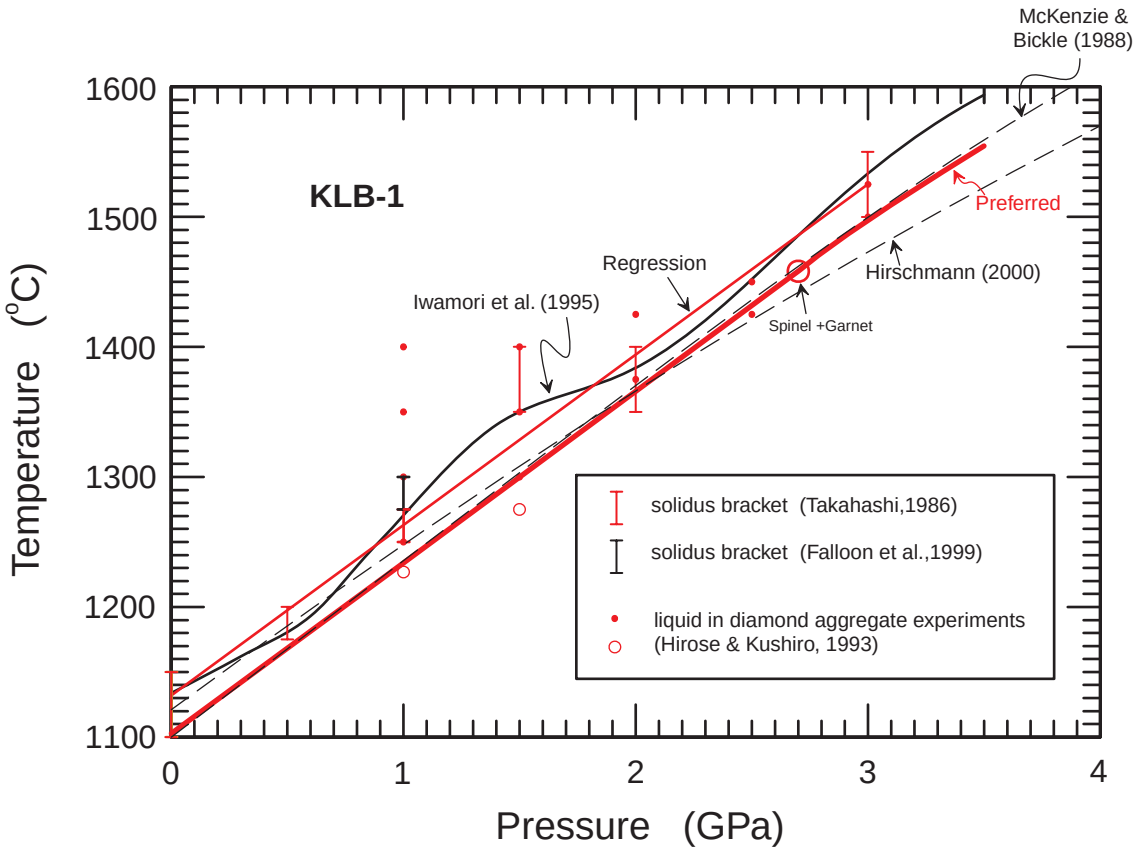

Figure 1. Experimental constraints on the anhydrous solidus for peridotite KLB-1. Vertical lines with terminations, solidus brackets of *Takahashi* [1986] and *Falloon et al.* [1999]; solid circles, experiments of *Hirose and Kushiro* [1993] that contain glass; small open circles, solidus estimated by extrapolation of *Hirose and Kushiro* [1993]T–F data to 0% liquid. The preferred solidus is discussed in the text.

KLB-1 using the piston-cylinder apparatus, and the *Takahashi* [1986] brackets have been parameterized by *Iwamori et al.* [1995] as shown in Figure 1. The solidus can also be constrained by extrapolation to $F = 0$ in isobaric experiments for which the melt fraction F has been estimated, as had been done by *Hirose and Kushiro* [1993], but this approach is not without problems [*Hirschmann*, 2000]. Both results are shown in Figure 1. The isobaric data of *Hirose and Kushiro* [1993] exhibit linear T–F relations, which we have extrapolated at 1.0 and 1.5 GPa with a minimum of three experimental data points used for these regressions. Inspection of Figure 1 shows that the solidus bracket of *Takahashi* [1986] can be ~80°C higher than that constrained by the T–F data of *Hirose and Kushiro* [1993], although the agreement is improved with melt fractions estimated by *Hirschmann* [2000]. Linear T–P regressions have been performed with pressure as the independent variable, and the solidus temperature brackets as dependent variables. When the solidus temperature is estimated by extrapolation of F to 0, as in the case for KLB-1, it is included as a dependent variable. Pressure is assumed to be without error. Linear regression of all KLB-1 data is insensitive to uncertainties in

Table 2. Spinel Lherzolite Solidus[a]

Composition	dT/dP (°C/GPa)	T_o, °C	R^2	2α, °C
CMAS	123 (6)	1200 (9)	0.98	28
KLB 1	131 (11)	1132 (73)	0.92	70
KLB 1 preferred	132	1102		
Tinaquillo Lherzolite TL	132 (8)	1123 (29)	0.99	16
MM 3	143 (38)	1111 (93)	0.78	36
Martian Mantle (DW)	140 (14)	1073 (33)	0.96	22
HK 66	143 (13)	1048 (23)	0.91	60
PHN 1611	133	1055		
Various: *McKenzie and Bickle* [1988]	132	1105		
Various: *Herzberg* [1983]	130	1140		
Various: *Hirschmann* [2000]	104-124			

[a] $T = (dT/dP)P + T_o$. Numbers in parentheses equal 1 standard deviation. 2 σ is error associated with equation constants in describing experimental brackets. CMAS: *Presnall et al.* [1979] and *Milholland and Presnall* [1998]. KLB1: *Takahashi* [1986] and *Hirose and Kushiro* [1993]. Tinaquillo Lherzolite: *Robinson et al.* [1998] and *Robinson and Wood* [1998]. MM3: *Baker et al.* [1995] and *Falloon et al.* [1999]. Martian Mantle DW: *Bertka and Holloway* [1994]. HK 66: *Takahashi and Kushiro* [1983] and *Hirose and Kushiro* [1993]. PHN 1611: *Kushiro* [1996]; determined at 1 and 3 GPa for $F = 0$ from experiments with assemblages of L + Ol + Opx + Cpx *Hirschmann* [2000] solidus is nonlinear.

extrapolation of F to 0 and yields a solidus temperature that is known to within ±70°C at the 2σ level (Table 2). *Hirschmann* [2000] came to the same conclusion and provided an excellent discussion of experimental uncertainties. Although solidus uncertainties are computed for temperature, we suspect that uncertainties in pressure calibration account for much of the uncertainty in solidus calibration.

[4] Experimental data on the solidus for the range of peridotite compositions listed in Table 1 are shown in Figure 2 and are compared to the peridotite solidus for the system CaO-MgO-Al_2O_3-SiO_2 (CMAS) [*Presnall et al.*, 1979; *Milholland and Presnall*, 1998]. Although some curvature is to be expected, we have fitted all solidus data to the linear equation:

$$T = (dT/dP)P + T_o. \quad (1)$$

Equation constants are listed in Table 2 for each peridotite composition within the spinel lherzolite stability field. Some of the data can also be fitted to nonlinear equations, but the error is reduced by only 2°C at the 2σ level. Inspection of Table 2 shows that regressions of the tightest experimental brackets yield an uncertainty of 16°–28°C (i.e., Tinaquillo Lherzolite, Dreibus and Wanke (DW), and CMAS compositions), considerably smaller than uncertainties associated with regressions on KLB-1 (±70°C) and HK-66 (±60°C). However, there is an important distinction between these two sets of experiments. Experiments on Tinaquillio Lherzolite, DW, and CMAS have never been reproduced, whereas KLB-1 and HK-66 were the subject of several investigations [*Takahashi and Kushiro*, 1983; *Takahashi*, 1986; *Hirose and Kushiro*, 1993; *Falloon et al.*, 1999]. We suggest that a solidus bracket of 10°–25°C, which is routinely reported for piston-cylinder experiments, is a measure of precision. A true test of experimental accuracy involves reproduction of experimental data over an extended period of time in different laboratories, and this yields an uncertainty of ±60 to 70°C for HK-66 and

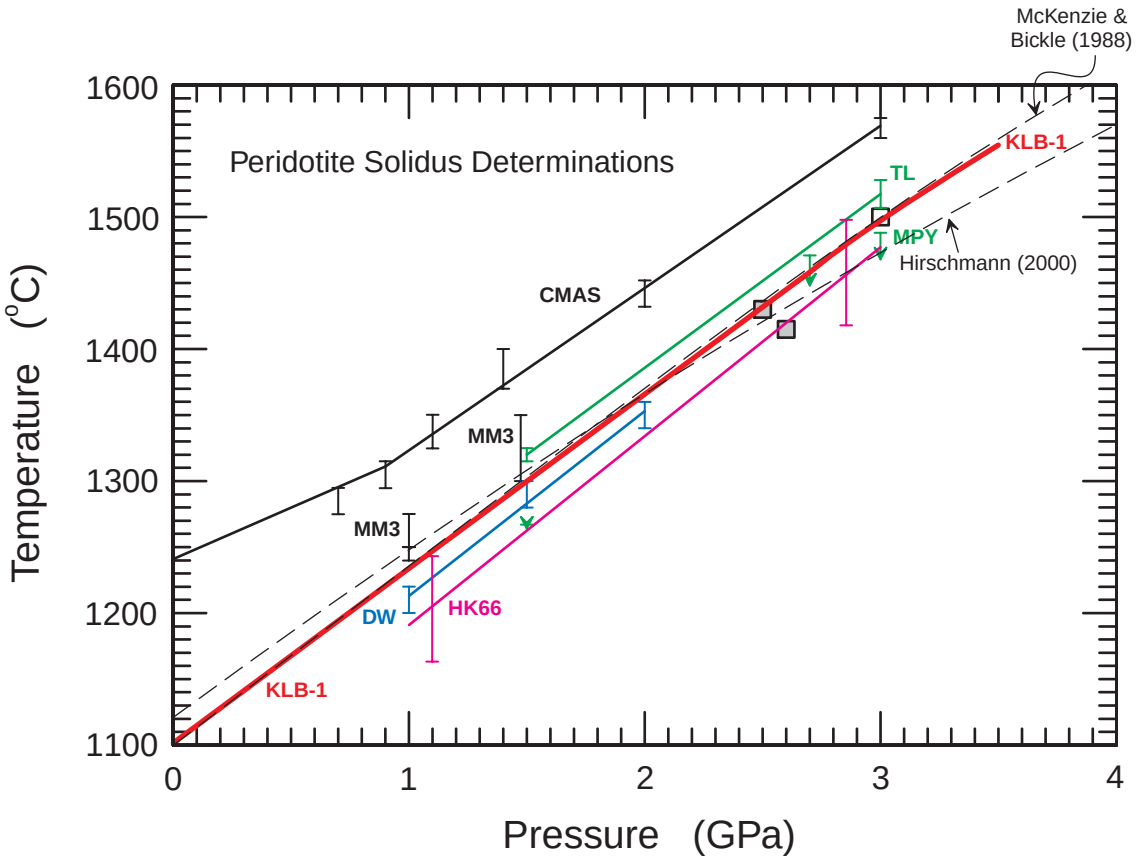

Figure 2. Experimental solidus brackets, and linear regressions for the range of peridotite compositions listed in Table 1. Data for MORB pyrolite (MPY) [*Robinson et al.*, 1998; *Robinson and Wood*, 1998] have not been regressed because they are half brackets in that a trace amount of melt occurs at each low-temperature terminus indicated by the arrow. Squares, Kettle River peridotite [*Walter*, 1998]; open square, supersolidus experiment; solid squares, subsolidus experiments; CMAS, CaO-MgO-Al_2O_3-SiO_2. See Table 1 for key to list of peridotite abbreviations.

KLB-1. More recent experimental work suggests that the error on accuracy can be lowered to about ±20°–30°C as indicated by the very good agreement between the solidus for Tinaquillo Lherzolite [*Robinson and Wood*, 1998] and KR-4003 [*Walter*, 1998] as shown in Figure 2.

[5] An obvious result of these comparisons is the similarity in *dT*/*dP* of the solidus for a wide range of spinel peridotite compositions (Figure 2, Table 2). The narrow experimental brackets on Tinaquillo Lherzolite [*Robinson et al.*, 1998; *Robinson and Wood*, 1998] yield 132±8°C/GPa (Table 2), similar to average slopes from compilations of experimental data on a variety peridotite compositions (130°C/GPa [*Herzberg*, 1983] and 132°C/GPa [*McKenzie and Bickle*, 1988]). Another noteworthy observation is the limited range of absolute solidus temperatures. At 1.5 GPa, regressed solidus temperatures differ by only 60°C for peridotite compositions that contain 7.18 to 17.9%

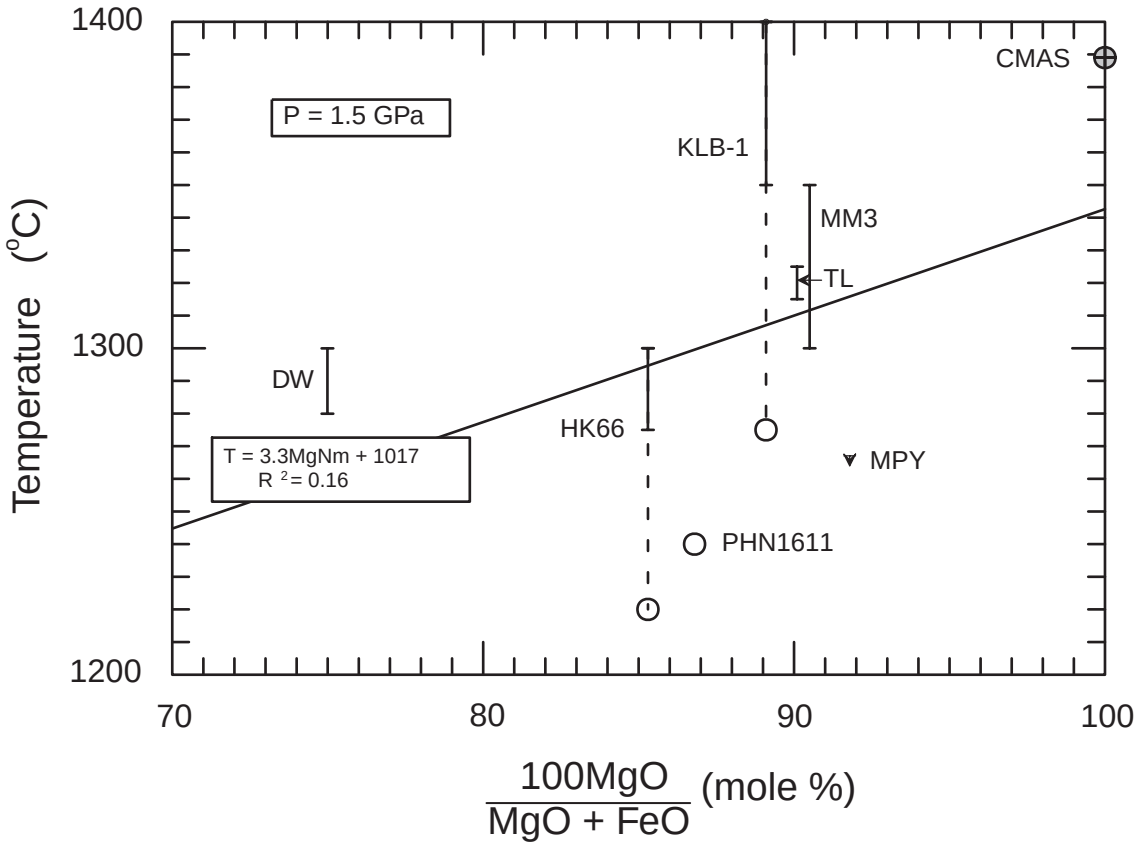

Figure 3. Solidus temperatures at 1.5 GPa as a function of Mg number for peridotite compositions listed in Table 1. Vertical lines with terminations, solidus brackets; open circles, solidus estimated by extrapolation of *T–F* data to 0% liquid using melt fractions reported by *Hirose and Kushiro* [1993] (see *Hirschmann* [2000] for discussion); CMAS = CaO-MgO-Al_2O_3-SiO_2. See Table 1 for key to list of peridotite abbreviations.

FeO (Mg # = 75.0 to 90.5; Table 1), similar to temperature uncertainties in the location of the solidus for KLB-1 and HK-66. Indeed, there is almost no correlation between Mg number and peridotite solidus temperature at 1.5 GPa as shown in Figure 3 (R^2 = 0.16). A better correlation exists between solidus temperature and total alkalis (Na_2O+K_2O), yielding R^2 = 0.48 (Figure 4), a conclusion reached also by *Hirschmann* [2000]. Alkalis exert the primary control on anhydrous peridotite solidus temperature, but this effect is diminished with increasing abundance of clinopyroxene [*Hirschmann*, 2000]. Some peridotites are unusually enriched in Cr_2O_3 (e.g., MPY, MM3, DW), and this tends to increase the solidus by ~20°C, although the paucity of data do not permit a rigorous statistical analysis. We expect that some H_2O and CO_2 in nominally anhydrous experiments may compromise the correlations in Figures 3 and 4.

[6] In addition to CaO and Cr_2O_3 the total alkali content of KLB-1 is the same as KR-4003 and only slightly higher than total alkalis in Tinaquillo Lherzolite. These compositional similarities permit us to use the

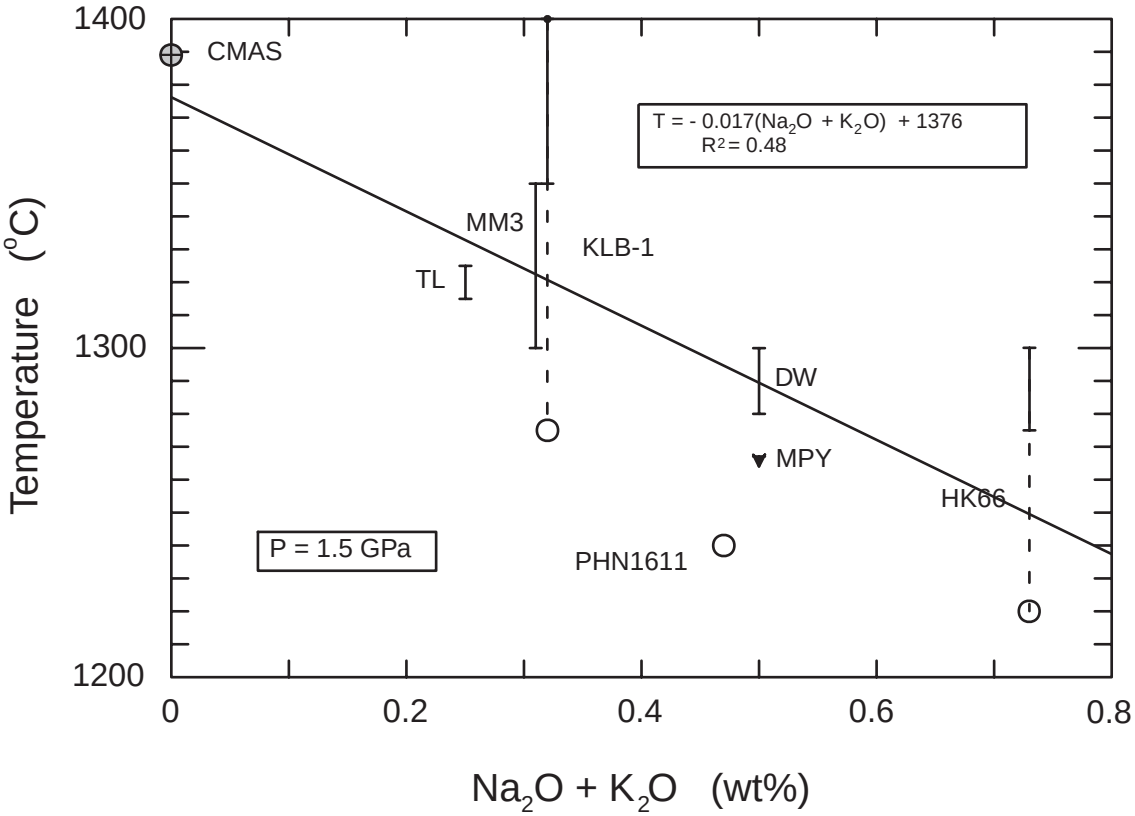

Figure 4. Solidus temperatures at 1.5 GPa as a function of alkali content. Vertical lines with terminations, solidus brackets; open circles, solidus estimated by extrapolation of T–F data to 0% liquid using melt fractions reported by *Hirose and Kushiro* [1993] (see *Hirschmann* [2000] for discussion); CMAS, CaO-MgO-Al_2O_3-SiO_2. See Table 1 for key to list of peridotite abbreviations.

tight brackets of *Robinson et al.* [1998], *Robinson and Wood* [1998], and *Walter* [1998] to narrow the uncertainties in the KLB-1 solidus to T–P values shown in Figures 1 and 2. Our preferred KLB-1 solidus in the spinel facies can be described by

$$T = (132^\circ\mathrm{C/GPa})P + 1102^\circ\mathrm{C} \qquad (2)$$

and is essentially identical to the solidus of *McKenzie and Bickle* [1988]. Our solidus differs from that of *Hirschmann* [2000] in having a larger slope, but it is similar to those for other peridotite compositions (Figure 2, Table 2). The slope offered by *Hirschmann* [2000] is lower in part because it is an average of an aggregate peridotite database. The larger slope for KLB-1 propagates to solidus temperatures that are ~30°C higher than those preferred by *Hirschmann* [2000] at 3 to 4 GPa.

[7] *Walter* [1998] observed spinel + garnet lherzolite at 2.6 GPa and 1415°C, and *Koga et al.* [1999] placed it at 2.4–2.5 GPa and 1360°C. Using the data of *Walter* [1998], *Koga et al.* [1999], *Nickel* [1986], and our solidus temperatures defined by (2), our preferred triple point for KLB-1 is at 1458°C and 2.7 GPa.

Table 3. KLB-1 Solidus Determinations[a]

Run	*P*, GPa	*T*, °C	Time, min	Capsule	Experimental Results	Microscopy
43.3160	5	1650	60	C	Ol, Gt, Cpx, QSil, Carb, IL, Su, Gl	TEM
26.1809*	5	1650	10	Re	(Ol, Gt, Cpx)	SEM
26.1809*	5	1650	10	Re	Ol, Gt, Cpx	TEM
54.3282	5	1650	8	Re	Ol, Gt, Cpx, Relict Opx	SEM
56.3302	5	1650	60	Re	Ol, Gt, Cpx, Relict Opx	SEM
27.1862*	5	1700	8	Re	(Ol, Gt, Cpx)	SEM
27.1862*	5	1700	8	Re	Ol, Gt, Cpx, QSil, Gl	TEM
25.1788*	5	1750	10	Re	(Ol, Gt, Cpx, Qsil)	SEM
44.3173	5.5	1675	60	C	Ol, Gt, Cpx, QSil, Carb, IL, Su, Gl	TEM
58.3324	7.5	1750	60	Re	Ol, Gt, Cpx	SEM
45.3179	7.5	1850	60	C	Ol, Gt, Cpx, QSil	SEM
18.1750*	9.7	1850	6	Re	(Ol, Gt, Cpx)	SEM
57.3310	9.7	1850	60	Re	Ol, Gt, Cpx	SEM
19.1749*	9.7	1900	8	Re	(Ol, Gt, Cpx)	SEM
53.3278	9.7	1900	8	Re	Ol, Gt, Cpx, QSil	SEM
23.1768*	9.7	1950	8	Re	(Ol, Gt, Cpx)	SEM
23.1768*	9.7	1950	8	Re	Ol, Gt, Cpx	TEM
51.3216	9.7	1950	87	Re	Ol, Gt, Cpx, QSil	SEM
52.3203	9.7	1950	60	Re	Ol, Gt, Cpx, QSil	SEM
24.1789*	9.7	2000	8	Re	[(Ol, Gt, Cpx, QSil)]	SEM

[a]Runs with asterisks were reported by *Zhang and Herzberg* [1994]. Runs wihtout asterisks are new data reported in this work. Experimental results in parentheses were reported by *Zhang and Herzberg* [1994]. Experimental results not in parentheses are observations in this work. SEM, scanning electron microscopy (backscatter); TEM, transmission electron microscopy. Ol, olviline; Gt, garnet; Cpx, clinopyroxene; QSil, quench Ol, Gt, Cpx from liquid; Carb, carbonate, IL, ilmenite; Su, sulfide (FeS); Gl, glass.

3. New Experiments on Peridotite KLB-1

3.1. Experimental Methods

[8] We attempted to reproduce the KLB-1 solidus reported in 1994 [*Zhang and Herzberg*, 1994] at 5–9.7 GPa. Special attention was focused on maintaining an experimental method that is fundamentally identical with the one we used in the earlier experiments [*Zhang and Herzberg*, 1994]. However, we also performed several additional experiments that were designed to explore the effects of variable run duration and sample container on the solidus. Several experimental products produced in this new work, together with archived samples from *Zhang and Herzberg* [1994], were examined with transmission electron microscopy (TEM) in addition to scanning electron microscopy (SEM).

[9] The reader can find a detailed description of our experimental method in the work of *Zhang and Herzberg* [1994]. Briefly, all experiments were performed with the Sumitomo multianvil press at Stony Brook using 14-mm assemblies, Re containers, straight lanthanum chromite heaters, and a high temperature-pressure calibration curve. The entire pressure assembly containing KBL-1 sample was fired at 1000°C in an argon atmosphere in order to remove all water.

[10] The criterion we applied to an experiment that was considered to be above the solidus was the observation of a quenched melt phase anywhere in the sample container. A subsoli-

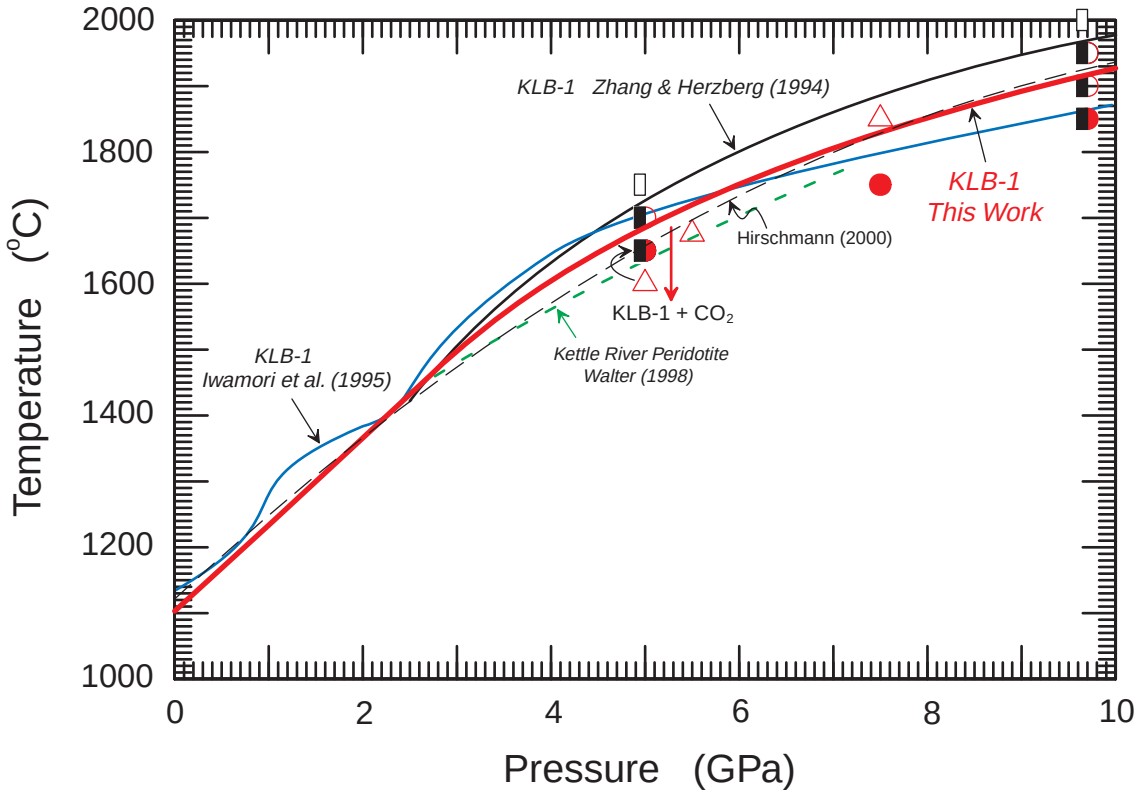

Figure 5. Solidus brackets for KLB-1, from data in Table 3. Solid symbols, all solid; open symbols, crystals + glass (or crystals quenched from liquid); red half circles, this work; black half squares, data from *Zhang and Herzberg* [1994]; triangles, KLB-1 contained in graphite containers. KLB-1 solidus in red at 0–2.7 GPa is from Figure 1. Note the solidus for KLB-1 at 4 GPa is 34°C higher than that suggested by *Hirschmann* [2000].

dus experiment was inferred from the absence of glass or crystals quenched from a liquid phase anywhere in the sample container. Given that the preparation of an experiment for SEM and TEM observation inevitably destroys parts of the charge which cannot be examined, it is possible a melt phase escaped our attention in a nominally subsolidus experiment. As shown below, this potential ambiguity can be tested by performing repeated experiments. A temperature gradient of ~50°C/mm exists near the hot spot where the thermocouple tip is positioned. All experimental brackets above the solidus contained an extremely small amount of melt, typically <2%, which was always confined to the vicinity of the thermocouple tip. Temperature gradients, which are a problem in experiments with a large melt fraction [*Zhang and Herzberg*, 1994; *Lesher and Walker*, 1988], do not contribute to ambiguities in these near-solidus experiments because (1) we have not attempted to determine equilibrium liquid compositions and (2) the absence of a melt phase anywhere in an experiment remains a subsolidus result even in the presence of a temperature gradient.

[11] Specimens for analytical TEM (ATEM) were cut in optically selected areas of doubly polished petrographic sections (20 μm thick) prepared from the near-solidus sam-

Table 4. Near-Solidus Phase Compositions for KLB-1 at 5 GPa

	Phase								
	Olivine	Olivine	Garnet	Garnet	Cpx	Cpx	Glass	Glass	Q Cpx
Method	ATEM[a]	Probe	ATEM	Probe	ATEM	Probe	ATEM	ATEM	ATEM
SiO_2	41.2	(40.2)	42.5	(42.83)	55.8	(54.37)	66.8	73.6	48.7
TiO_2	-	(0.02)	0.48	(0.18)	-	(0.10)	1.49	-	0.76
Al_2O_3	0.22	(0.35)	22.7	(22.0)	3.61	(4.05)	14.0	23.2	9.13
Cr_2O_3	(0.10)	0.29	(1.22)	2.32	(0.36)	0.50	-	-	-
FeOt	9.82	(9.96)	6.67	(6.20)	5.61	(6.01)	6.45	1.28	9.82
MnO	0.13	(0.12)	0.23	(0.17)	0.11	(0.11)	0.13	-	0.22
Mgo	47.9	(48.13)	21.0	(21.5)	26.5	(25.54)	2.09	1.35	13.8
CaO	0.27	(0.29)	5.17	(4.69)	7.46	(8.5)	6.56	0.41	16.3
Na_2O	-	(0.13)	-	(0.05)	0.41	(0.65)	1.14	0.14	1.2
K_2O	-	-	-	-	-	-	1.3	-	-
NiO	(0.36)	0.45	-	(0.06)	0.12	(0.11)	-	-	-
Total	100	99.94	99.97	100	99.98	99.94	99.96	99.98	99.93
Mg #	89.7	89.6	84.9	86.1	89.4	88.3	36.6	65.4	71.4

[a]ATEM, this work; Probe, electron microprobe determination [*Herzberg and Zhang*, 1996]; Q Cpx, Quench Cpx; numbers in parentheses indicate preferred concentrations from minimized residuals KLB-1 [*Herzberg et al.*, 1990] is 62.9% olivine + 10.1% garnet + 27.0% Cpx.

ples. Petrographic sections were then ion-thinned (5-kV argon beam) to electron transparency. A Philips CM30 electron microscope, operating at 300 kV and equipped with an energy dispersive X-ray (EDX) spectrometer (Noran-Voyager), was used to examine the specimens. This EDX spectrometer has a germanium detector and an ultra-thin window that allows the detection and quantification of oxygen. Microanalyses were performed in the ATEM mode on scanned areas (typically from 0.01 to 0.25 μm^2). We used a method developed by *Van Cappelen and Doukhan* [1994] for the thickness correction. This method yields major element oxide compositions precise to 1% absolute (for more details on these ATEM techniques, see *Raterron et al.* [1999]).

3.2. Experimental Results

[12] Experimental results are tabulated in Table 3 and shown in Figure 5. Included for comparison are near-solidus experimental results from our previous work [*Zhang and Herzberg*, 1994]. Our new solidus brackets are lower in temperature than our old ones by ~50° at 5 GPa and 70° at 9.7 GPa.

[13] We observed no melt phase in any of the four separate experiments (Re) conducted at 1650°C and 5 GPa with either SEM or TEM (Table 3); this excellent reproducibility indicates that we have not missed a melt phase during sample preparation and that these are true subsolidus results. At 5 GPa the new solidus is bracketed between 1650° and 1700°C; this compares with our previous bracket of 1700°–1750°C [*Zhang and Herzberg*, 1994]. This difference arises from difficulties we previously had in identifying a melt phase when it is present at low melt fractions near the solidus. In our experiment at 1700°C and 5 GPa (run 27.1862) a melt phase was not directly observed in SEM, but on reexamination using TEM it was observed as glass and quench clinopyroxene (Cpx) at triple junctions. Electron microprobe [*Herzberg and Zhang*, 1996] and ATEM analyses of equilibrium olivine, garnet, and Cpx

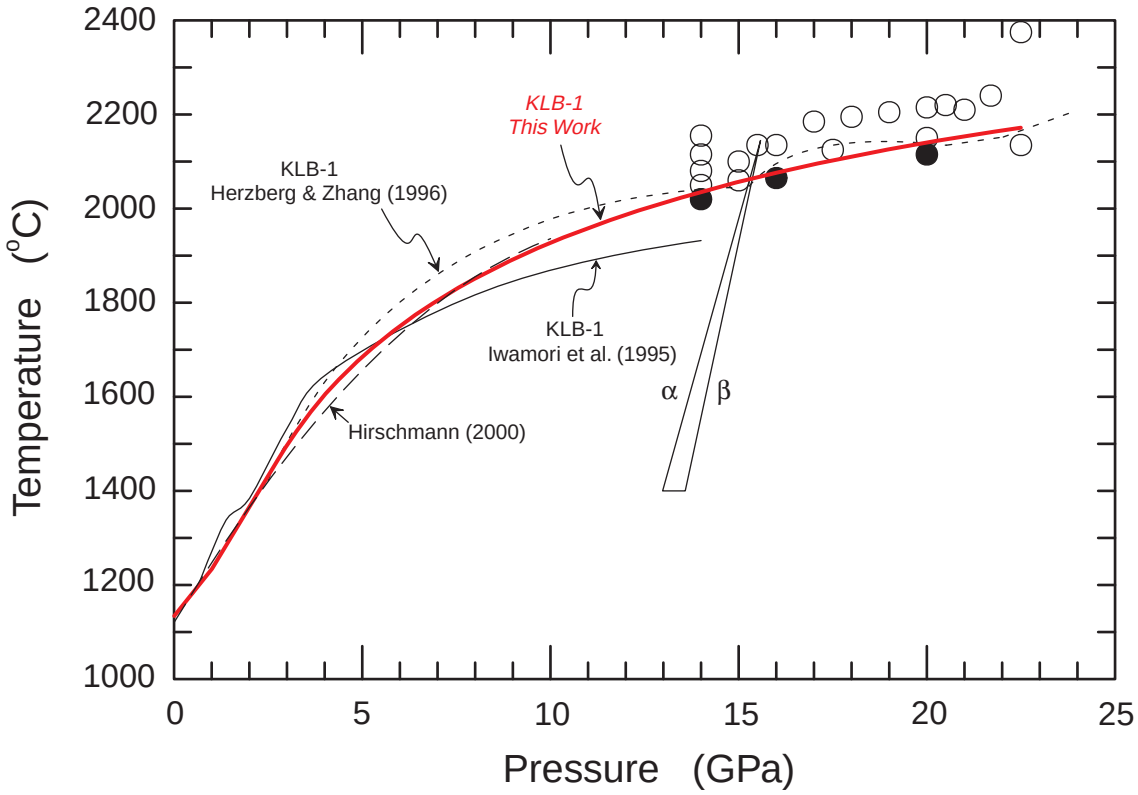

Figure 6. Solidus brackets for KLB-1 at 14 GPa [*Herzberg et al.*, 1990] and 15–20 GPa [*Zhang and Herzberg*, 1994; *Herzberg and Zhang*, 1996]. KLB-1 solidus at 0–10 GPa is from Figure 5. Open circles, experiments that contained a quenched melt phase; solid circles, experiments that showed no evidence of a melt phase anywhere in the capsule. The experiment at 2135°C and 22.5 contains a quenched melt phase but plots below the solidus because of a large temperature gradient. The effects of temperature gradients on solidus estimates were examined for experiments containing liquid by locating the relative position of the thermocouple tip [*Zhang and Herzberg*, 1994; *Herzberg and Zhang*, 1996], and the agreement with this work is very good. The anhydrous solidus recommended by *Hirschmann* [2000] is essentially identical to that of KLB-1 at 1 atmosphere to 10 GPa and at this T–P scale of observation.

crystals located near the solidus are in very good agreement as shown in Table 4. However, at triple junctions, quench Cpx analyzed by ATEM is low in Mg number and high in Al_2O_3. Glass at triple junctions is unusually high in SiO_2 (67–74%), indicating extensive modification of the melt composition during the quench and precluding a mass balance estimate of the melt fraction.

[14] In the subsolidus experiments at 1650°C and 5 GPa, olivine grains are uniformly gray when viewed with backscatter SEM. However, in experiments at 1700°C and 5 GPa that contained a melt phase, olivine grain boundaries at triple junctions show darkening in grayscale variations when observed in backscatter SEM images owing to the partitioning of FeO into the melt phase. These SEM grayscale variations in olivine can be used as a criterion for recognizing melting even when a distinct melt phase cannot be directly observed owing to its low mass fraction or to melt migration. This permits a subsolidus result to

be identified when the SEM is the only microscope at the experimentalist's disposal, as long as the melt phase is anhydrous (a caveat we discuss below).

[15] At 9.7 GPa the new KLB-1 solidus is bracketed between 1850° and 1900°C, but there is paucity of melt at 1900°C. Our previous bracket placed the solidus between 1950° and 2000°C. The reason for this discrepancy is not related to the problem in identifying a melt phase; both SEM and TEM observations on our old experiment at 1950°C and 9.7 GPa (run 23.1768) show no melt phase anywhere in the experiment. We are therefore puzzled by this discrepancy because there is no obvious experimental explanation and conclude that it is a reflection of experimental uncertainty. The new solidus offered in Figure 5 satisfies our old and new data at 9.7 GPa to within ±68°C (2σ), which is similar to the uncertainty in locating the KLB-1 solidus at 1–3 GPa (Figure 1, Table 2). Unpublished data on KLB-1 in the 5 to 10 GPa range determined at the Tokyo Institute of Technology were parameterized by *Iwamori et al.* [1995], and the results agree with our new solidus to within ±60°C (Figure 5).

[16] In 1990 we reported a narrow solidus bracket of 2020°–2050°C for KLB-1 at 14 GPa using a 10-mm pressure assembly [*Herzberg et al.*, 1990]. In 1994 we extended the 14-GPa solidus to the 15–22.5 GPa range in experiments using the same experimental method [*Zhang and Herzberg*, 1994] and were able to bracket the solidus at 20 GPa by 35°C (Figure 6). These tight brackets and excellent reproducibility, shown in Figure 6 [*Zhang and Herzberg*, 1994], were generated in the laboratory over an extended interval of time and point to the unexpected result of improved accuracy over the lower-pressure results. We suggest that the uncertainty of ±68°C for the 14-mm multi-anvil assembly can be improved to about ±20°–30°C, comparable to that which is obtainable with the piston-cylinder apparatus. These data at 14.0–22.5 GPa have been regressed with our new 5-GPa solidus bracket, both old and new data at 9.7 GPa, and with our 2.7-GPa triple point. These results for the garnet peridotite solidus are described by

$$T = 1086 - 5.7P + 390\ln(P) \quad (3)$$

to within ±68°C (Figure 6) for the entire 2.7–22.5 GPa range, pressures that cover both upper mantle and transition zone. The anhydrous solidus recommended by *Hirschmann* [2000] at 1 atm to 10 GPa is essentially identical to that of KLB-1 at this T–P scale of observation, but the Tokyo solidus at 14 GPa is 100°C lower.

[17] Several experiments were designed to explore the effect of run duration and sample container on the solidus. The solidus was found to be unaffected by durations that ranged from 8 to 60 min, but it was lowered when the rhenium sample container was replaced with graphite (Figure 5). Two experiments were run with graphite containers at 5.0 and 5.5 GPa and at temperatures below the solidus as defined by experiments with rhenium (run 43.3160 and 44.3173). No evidence for melting was observed in SEM. However, TEM images show triple junctions with complex assemblages of SiO_2 glass, quench olivine, pyroxene, and garnet with low Mg numbers, ilmenite, and $CaCO_3$ with minor FeS (Figure 7). The amount of melt was probably <1%, and the amount of $CaCO_3$ increases toward the contact with graphite, demonstrating that the container is the source of carbon. We interpret the carbonate as a quench phase from a melt that contained dissolved CO_2, which originated in a reaction of the type:

$$Fe_2O_3(\text{silicate}) + C = CO_2(\text{melt}) + 2FeO. \quad (4)$$

If this interpretation is correct, it implies some Fe_2O_3 was present in KLB-1 during initial drying of our sample + assembly in an Ar

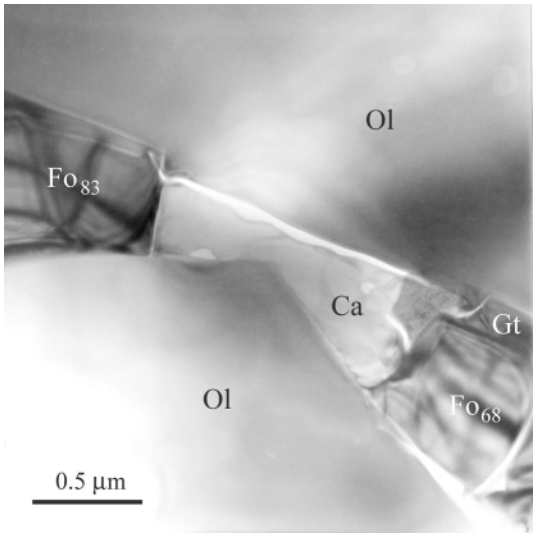

Figure 7. TEM image of experiment on KLB-1 contained in a graphite capsule at 1600°C and 5 GPa (run 43.3160; Table 3). Phases at triple junctions are $CaCO_3$ (Ca) and quench olivine with forsterite contents of 68–83%.

atmosphere at 1000°C and that our experimental method should have included sintering of KLB-1 at a lower oxygen fugacity. Whatever the correct interpretation may be, our experiments clearly show that graphite sample containers are not without problems. Also, we can expect substantial lowering of the solidus temperature for C-contained samples that have not been fired to expel H_2O. Our new solidus for KLB-1 is now ~50°C higher than that for Kettle River peridotite at 5 GPa [*Walter*, 1998] (Figure 5), a difference that may reflect experimental uncertainties or the relatively lower K_2O in KLB-1 (Table 1). However, the experiments on Kettle River peridotite (fired) were conducted with graphite capsules, and we anticipate that some nominally subsolidus experiments reported by *Walter* [1998] may also contain a CO_2-rich melt phase if observed in TEM. The implication is that a truly anhydrous solidus may only be accurately located when the sample is encapsulated in an unreactive substance like rhenium.

Acknowledgments

[18] The high-pressure experiments were performed at the Stony Brook High Pressure Laboratory, which is part of the NSF Science and Technology Center for High Pressure Research (EAR 89-20239). This is SUNY Mineral Physics Institute Publication Number 293. Michael Walter and an anonymous reviewer are thanked for detailed reviews. Thanks are extended to Marc Hirschmann for a preprint of his G-Cubed review on the peridotite solidus and to Bill White who provided us with the link to Hirschmann's work.

References

Baker, M. B., M. M. Hirschmann, M. S. Ghiorso, and E. M. Stolper, Compositions of near-solidus peridotite melts from experiments and thermodynamic calculations, *Nature*, *375*, 308–311, 1995.

Bertka, C. M., and J. R. Holloway, Anhydrous partial melting of an iron-rich mantle I: subsolidus phase assemblages and partial melting phase relations at 10 to 30 kbar, *Contrib. Mineral. Petrol.*, *115*, 313–322, 1994.

Falloon, T. J., D. H. Green, L. V. Danyushevsky, and U. H. Faul, Peridotite melting at 1.0 and 1.5 GPa: An experimental evaluation of techniques using diamond aggregates and mineral mixes for determining near-solidus melts, *J. Petrol.*, *40*, 1343–1375, 1999.

Herzberg, C. T., Solidus and liquidus temperatures and mineralogies for anhydrous garnet-lherzolite to 15 GPa, *Phys. Earth Planet. Inter.*, *32*, 193–202, 1983.

Herzberg, C., and T. Gasparik, H. Sawamoto, Origin of mantle peridotite: Constraints from melting experiments to 16.5 GPa, *J. Geophys. Res.*, *95*, 15,779–15,803, 1990.

Herzberg, C., and J. Zhang, Melting experiments on anhydrous peridotite KLB-1: Compositions of magmas in the upper mantle and transition zone, *J. Geophys. Res.*, *101*, 8271–8295, 1996.

Hirose, K., and I. Kushiro, Partial melting of dry peridotites at high pressures: Determination of compositions of melts segregated from peridotite using aggregates of diamond, *Earth Planet. Sci. Lett.*, *114*, 477–489, 1993.

Hirschmann, M. M., Mantle solidus: Experimental constraints and the effects of peridotite composition, *Geochem. Geophys. Geosyst.*, (Article), 2000GC000070 [11,012 words], 2000.

Iwamori, H., D. McKenzie, and E. Takahashi, Melt generation by isentropic mantle upwelling, *Earth Planet. Sci. Lett.*, *134*, 253–266, 1995.

Koga, K. T., N. Shimizu, and T. L. Grove, Disequilibrium trace element redistribution during garnet to spinel facies transformation, in *7th International Kimberlite Conference*, edited by J.J. Gurney, pp. 444–451,National Book Printers, Cape Town, South Africa, 1999.

Kushiro, I., Partial melting of a fertile mantle peridotite at high pressures: An experimental study using aggregates of diamond, in *Earth Processes: Reading the Isotopic Code, Geophys. Monogr. Ser.*, vol. 95, edited by A. Basu and S. Hart, pp. 109–122,AGU, Washington, D. C., 1996.

Lesher, C. E., and D. Walker, Cumulate maturation and melt migration in a temperature gradient, *J. Geophys. Res.*, *93*, 10,295–10,311, 1988.

McKenzie, D., and M. J. Bickle, The volume and composition of melt generated by extension of the lithosphere, *J. Petrol.*, *29*, 625–679, 1988.

Milholland, C. S., and D. C. Presnall, Liquid phase relations in the CaO-MgO-Al_2O_3-SiO_2 system at 3.0 GPa: The aluminous pyroxene thermal divide and high-pressure fractionation of picritic and komatiitic magmas, *J. Petrol.*, *39*, 3–27, 1998.

Nickel, K. G., Phase equilibria in the system SiO_2-MgO-Al_2O_3-CaO-Cr_2O_3 (SMACCR) and their bearing on spinel/garnet lherzolite relationships, *Neues Jahrb. Mineral. Abh.*, *155*, 259–287, 1986.

Presnall, D. C., J. R. Dixon, T. H. O'Donnell, and S. A. Dixon, Generation of mid-ocean tholeiites, *J. Petrol.*, *20*, 3–35, 1979.

Raterron, P., M. A. Carpenter, and J. C. Doukhan, Sillimanite mullitization: ATEM investigation and point defect model, *Phase Transitions*, *68*, 451–500, 1999.

Robinson, J. A. C., and B. J. Wood, The depth of the spinel to garnet transition at the peridotite solidus, *Earth Planet. Sci. Lett.*, *164*, 277–284, 1998.

Robinson, J. A. C., B. J. Wood, and J. D. Blundy, The beginning of melting of fertile and depleted peridotite at 1.5 GPa, *Earth Planet. Sci. Lett.*, *155*, 97–111, 1998.

Takahashi, E., Melting of a dry peridotite KLB-1 up to 14 GPa: Implications on the origin of peridotitic upper mantle, *J. Geophys. Res.*, *91*, 9367–9382, 1986.

Takahashi, E., and I. Kushiro, Melting of a dry peridotite at high pressures and basalt magma genesis, *Am. Mineral.*, *68*, 859–879, 1983.

Van Cappelen, E., and J. C. Doukhan, Quantitative transmission X-ray microanalysis of ionic compounds, *Ultramicroscopy*, *53*, 343–349, 1994.

Walter, M. J., Melting of garnet peridotite and the origin of komatiite and depleted lithospere, *J. Petrol.*, *39*, 29–60, 1998.

Zhang, J., and C. Herzberg, Melting experiments on anhydrous peridotite KLB-1 from 5.0 to 22.5 GPa, *J. Geophys. Res.*, *99*, 17,729–17,742, 1994.